

One-Step Preparation of Fluorographene: A Highly Efficient, Low-Cost, and Large-Scale Approach of Exfoliating Fluorographite

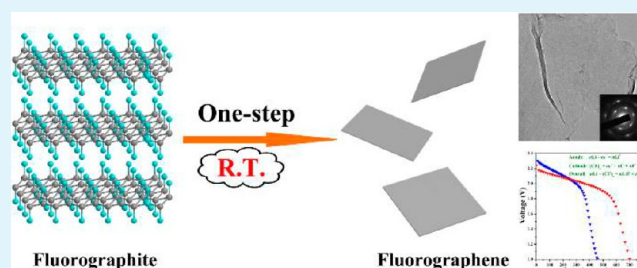
Yang Yang, Guolin Lu, Yongjun Li,* Zhanzhan Liu, and Xiaoyu Huang*

Key Laboratory of Organofluorine Chemistry and Laboratory of Polymer Materials, Shanghai Institute of Organic Chemistry, Chinese Academy of Sciences, 345 Lingling Road, Shanghai 200032, People's Republic of China

Supporting Information

ABSTRACT: Fluorographene, a cousin of graphene, not only inherits the excellent mechanical properties of graphene but also has great unique application potential in high-performance devices and materials, such as lubricating agents, digital transistors, nanocomposites, and energy-storage devices. However, large-scale preparation of fluorographene remains a great challenge. Herein, an easy-operating, highly scalable, and low-cost approach was reported for the preparation of fluorographene using commercially available fluorographite as the starting material. In this procedure, fluorographite turned into few-layer fluorographene through a rapid exfoliation process with Na_2O_2 and HSO_3Cl as exfoliating agents. The whole preparation process was performed in air and without heating, sonication, and protective gas. The obtained fluorographene was characterized by Fourier transform infrared spectroscopy, Raman spectroscopy, ^{19}F nuclear magnetic resonance spectroscopy, X-ray diffraction, thermogravimetric analysis, atomic force microscopy, and transmission electron microscopy, and it possesses a hexagonal polycrystalline structure. Fluorographene and fluorographite were employed as cathode materials of the primary lithium battery, and it was found that the specific discharge capacity of the battery using fluorographene was improved remarkably compared to that using fluorographite. Cyclic voltammetry results also showed that specific capacitances of fluorographene were dozens of times higher than that of fluorographite. It is clear that electrochemical properties of fluorographene are significantly improved against fluorographite.

KEYWORDS: fluorographite, fluorographene, exfoliation, one-step preparation, low cost, large scale



1. INTRODUCTION

Since graphene was prepared from highly oriented pyrolytic graphite,¹ this kind of 2D nanomaterial has become one of the biggest hotspots in materials science because of its unique properties and characteristics.^{2,3} The research on graphene has made for significant progress in many fields such as nanoelectronics, chemistry, biology, and nanocomposite material science due to its excellent electrical, electronic, mechanical, and optical properties.^{4–13} Besides graphene, graphene-derived 2D nanomaterials are also attracting growing interests for their novel properties different from graphene. Fluorographene (FG), a new derivative of graphene that was just discovered recently,^{14–16} is an exciting new material because it both inherits the excellent mechanical properties of graphene and has its distinctive performances.¹⁷ As FG has unique properties, it exhibits potential value in future applications. It can be predicted that there will be considerable demand for FG in future industrial occasions.

In recent years, the preparation methods of graphene have made gratifying advancements. Multifarious approaches such as chemical vapor deposition, epitaxial growth, liquid phase exfoliation, and exfoliation of graphite oxide following chemical reduction, and so on,^{17–21} have been developed to produce graphene. Today, we can select the most appropriate way to

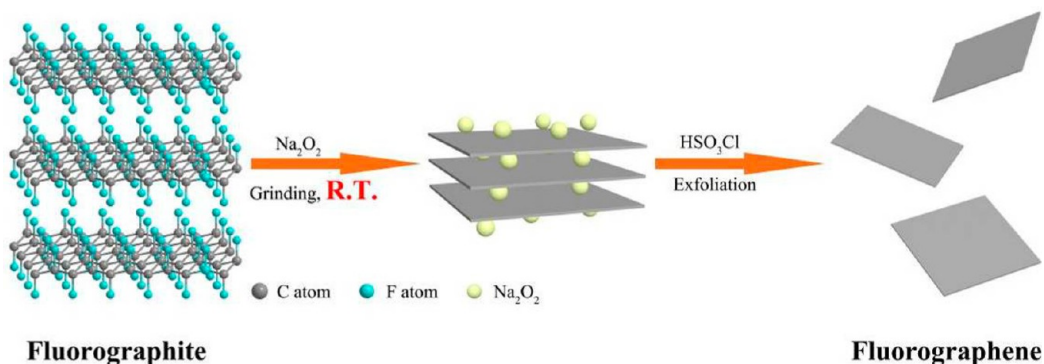
obtain graphene according to the demand of application and cost. However, in comparison with graphene, the preparation of FG is relatively difficult. At this time, three types of preparation methods are mainly employed to obtain FG as follows: (1) reacting graphene with XeF_2 or F_2 . FG or partially fluorinated graphene have been synthesized by exposing graphene in XeF_2 or F_2 atmosphere.^{14,16,17,22} Although high-quality FG can be prepared through this method, the higher cost constraints the large-scale production of FG. (2) Exfoliation of fluorographite. Mechanical exfoliation of fluorographite has been realized to prepare FG.²³ Obviously, it is quite difficult to produce FG in a large scale by this way. A liquid-phase exfoliation method for preparing FG has also been achieved in some solvents such as sulfolane or *N*-methyl-2-pyrrolidone.^{24,25} Nevertheless, the former solvent is highly toxic and the latter process needs a considerable period of ultrasonic time. In addition, chemical exfoliation of fluorographite by using ion liquid, for example 1-butyl-3-methylimidazolium bromide, as an exfoliating agent under ambient conditions was utilized to obtain FG,²⁶ but it is hard to rinse the ion liquid away completely. (3) Fluorination

Received: October 30, 2013

Accepted: December 7, 2013

Published: December 8, 2013

Scheme 1. Preparation Process of Fluorographene via Fluorographite



- ✓ No heating and protective gas
- ✓ Low cost of raw materials and preparation
- ✓ Suitable for large-scale preparation

of graphene oxide (GO). Very recently, FG has been prepared by fluorination of GO with HF or F₂.^{27,28} However, FG sheets obtained by this approach show an irregular atomic arrangement compared to the theoretical crystal structure of FG. It is clear that all aforementioned methods have their respective inadequacies, thus it is still necessary to develop a new convenient method for preparing FG.

In the current work, we exhibited an easy-operating, highly scalable, and low-cost method for rapid preparation of few-layer FG by using sodium peroxide and chlorosulfonic acid as exfoliating agents (Scheme 1). The instruments used in this method were quite simple, and the full preparation process needed only a one-step reaction. Therefore, the operating steps are easy without heating, sonication, and protective gas, and the products can be obtained in a large scale. Furthermore, all the experimental reagents used in this strategy are industrial bulk materials, which are relatively cheap, so this procedure is a low-cost method. The obtained FG was also proven to possess outstanding electrochemical properties with a much higher specific discharge capacity compared to fluorographite and a very high specific capacitance dozens of times of that of fluorographite. In brief, this work paved a new way for the convenient preparation of FG and laid a foundation for its future large-scale applications.

2. EXPERIMENTAL SECTION

2.1. Reagents. Fluorographite (F% > 56%, Shanghai CarFluor Chemicals Co. Ltd.), chlorosulfonic acid (HSO₃Cl, SinoPharm, 99.0%), sodium peroxide (Na₂O₂, SinoPharm, 95%), *N*-methyl-2-pyrrolidone (NMP, Alfa Aesar, 99.0%), and methanol (Aldrich, 99.%) were used as received.

2.2. Preparation of FG. In a typical experiment, 0.1 g of fluorographite powder and 1 g of Na₂O₂ were mixed homogeneously through adequate grinding in a corundum crucible. Next, 5 mL of HSO₃Cl was added into the mixture dropwise under stirring. **Caution!** As the reaction of Na₂O₂ and HSO₃Cl was quite violent and lots of light and heat were released during the dropping process, this addition operation of HSO₃Cl should be carried out slowly. After the reaction system was cooled down, the mixture was diluted with 100 mL of deionized water followed by filtering the suspension through a 0.22 μm poly(vinylidene fluoride) membrane. The solid was washed with

deionized water and dried at 60 °C overnight to afford a black powder of FG.

2.3. Characterization of FG. For transmission electron microscopy (TEM) and high-resolution transmission electron microscopy (HRTEM, JEOL JEM-2100F, acceleration voltage: 200 kV) observations, 1 mg of dried powder was dispersed in 3 mL of NMP or methanol undergoing a two-hour sonication. After standing for 48 h, the supernatants were dropped onto carbon mesh grids (230 mesh) for observation. For atomic force microscopy (AFM, VEECO Dimension 3100) measurement, the obtained supernatant in methanol was dropped onto silicon pellets and then dried in a far-infrared dryer. The supernatants in NMP were used for ¹⁹F NMR (Varian Mercury 300, 300 MHz). Discharging experiments were carried out on a BTS-5V/10mA battery test system at room temperature. To prepare the electrode, a mixture of 85% FG or fluorographite, 10% acetylene black, and 5% poly(vinylidene fluoride) binder was homogeneously dispersed in NMP with stirring. The resulting clay was pressed onto an Cu grid collector and then dried in vacuo at 120 °C for 12 h. The coin-type cell was fabricated by stacking FG or fluorographite electrode, separator, and lithium in a glovebox under Ar. The electrolyte was 1 M LiPF₆ in an ethylene carbonate/dimethyl carbonate solution (v/v = 1:1). The cyclic voltammetry measurements were performed on a CHI 660D electrochemical workstation (Chenhua, Shanghai); 3 mg of dried powder was dispersed in 3 mL of methanol with a one-hour sonication, and 50 μL of the mixture was dropped onto a glassy carbon electrode. For FT-IR (Nicolet AVATAR-360), Raman (Thermo Scientific DXR, semiconductor laser, wavelength: 532 nm), X-ray diffraction (XRD, Panalytical X'Pert Pro) and thermogravimetric analysis (TGA, TA Q500), the powder samples were directly used without any further treatment.

3. RESULTS AND DISCUSSION

In a previous study, few-layer graphene was produced with using HSO₃Cl and H₂O₂ as exfoliating agents.²⁹ Inspired by this report, we first tried to prepare FG from fluorographite by using HSO₃Cl and H₂O₂ as exfoliating agents, but TEM observations (Figure 1g,h) showed that the obtained sheets were quite thick with poor transparency, which meant that this experimental result was unsatisfactory. After careful analysis, we think that because both fluorographite and FG are full of C–F bonds, they are both hydrophobic materials. However, 30% aqueous H₂O₂ contains a large amount of water so that fluorographite originally dispersed homogeneously in HSO₃Cl

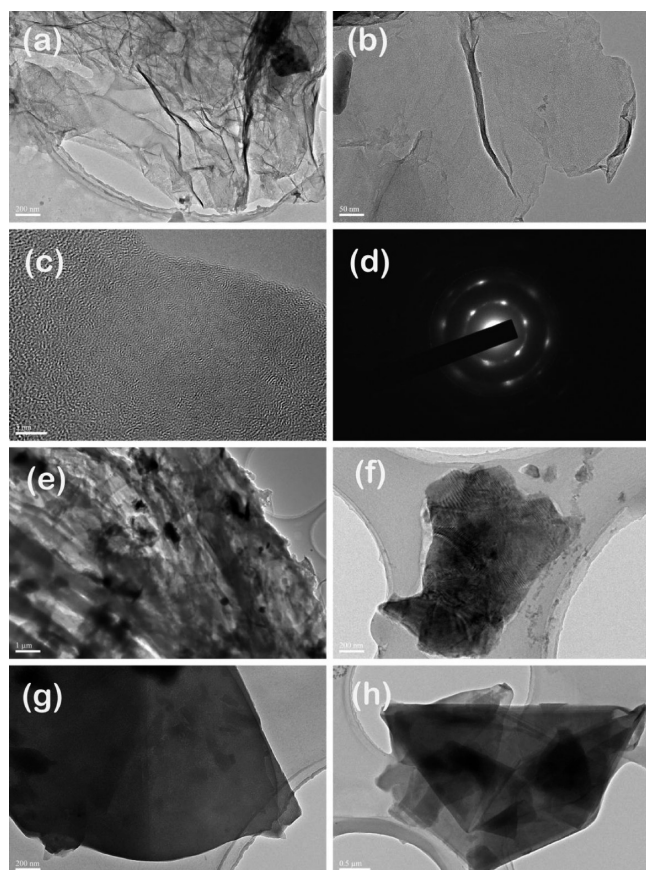


Figure 1. (a, b) TEM images of fluorographene sheets. (c) HRTEM image of a fluorographene sheet. (d) SAED pattern of fluorographene. (e, f) TEM images of pristine fluorographite. (g, h) TEM images of the unsatisfactory thick sheets obtained by using HSO_3Cl and H_2O_2 as exfoliating agents.

would separate out from the reaction system and float over the liquid phase. This phenomenon must not be favorable for the exfoliation driven by the local heat released from the reaction of HSO_3Cl and H_2O_2 . Considering the above results, Na_2O_2 was chosen instead of H_2O_2 because Na_2O_2 has two prominent

advantages compared to H_2O_2 : first, Na_2O_2 is a solid powder and does not contain any water; second, as Na_2O_2 is a strong base, the reaction of Na_2O_2 with HSO_3Cl is much more violent than that of H_2O_2 , and there will be greater energy produced in this reaction. That is why a lot of flare was generated during the reaction process as we mentioned in the Experimental Section. According to this line of thought, few-layer FG was successfully acquired by using HSO_3Cl and Na_2O_2 as exfoliating agents.

The acquired FG sheets were first identified by their morphology and crystal structure from TEM observations. Figure 1a,b clearly shows the typical corrugated morphology of transparent FG sheets, which directly proves the gaining of few-layer FG. For comparison, TEM images of pristine fluorographite were also taken as shown in Figure 1e,f. Unlike FG sheets, pristine fluorographite pieces were opaque, so we can easily see this thickness difference between FG and fluorographite. Figure 1c,d exhibits a HRTEM image and the selected area electron diffraction (SAED) pattern of a FG sheet. The SAED pattern indicated that FG has a diminished hexagonal structure along with amorphous halos.¹⁷ It meant that FG showed a hexagonal polycrystalline structure whereas pristine graphene usually shows a hexagonal single crystal structure. This is because the violent exfoliation process also caused many new wrinkles on FG layers, which led to many more crystal orientations.

AFM was then performed to obtain the height information of FG sheets. As shown in Figure 2, we can see that the thickness of a FG sheet was about 4.7 nm (the green scanning line). Taking into account that the thickness of monolayer graphene or graphene oxide examined by AFM measurement was about 1 nm,^{30–32} it can be concluded that the obtained FG sheets were few-layer ones. The red scanning line shows the morphology of three FG stacked sheets with a total height of 15.5 nm.

Raman spectroscopy, which has been employed for accurate identification of the layers of graphene sheets,³³ was also run to examine the exfoliation degree of fluorographite. Figure 3 shows Raman spectra of pristine fluorographite and the obtained FG. Compared to that of pristine fluorographite, Raman spectrum of FG exhibited a sharp 2D band at 2665 cm^{-1} and its intensity has remarkably improved. The changes in the shape and intensity of this 2D band reflected the formation

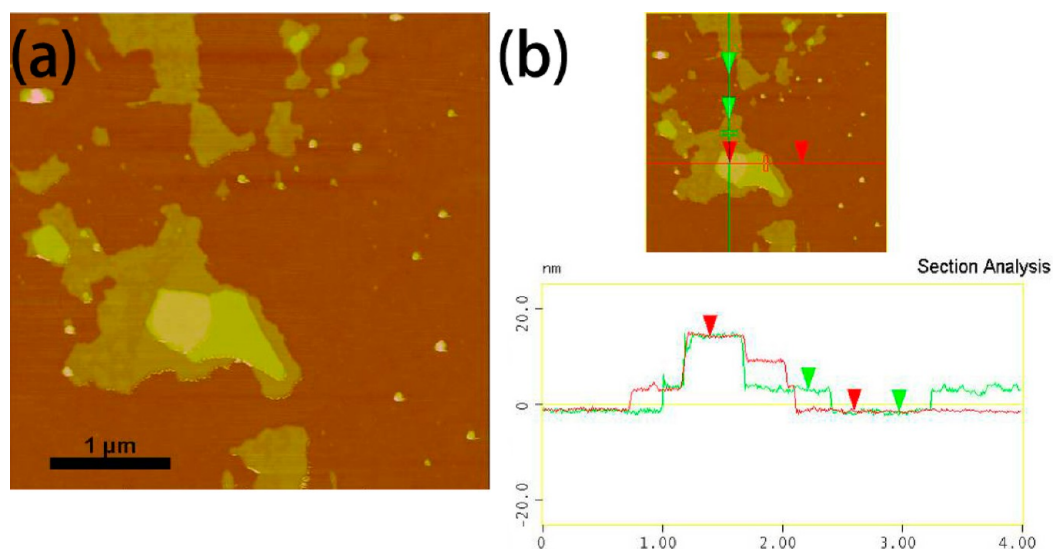


Figure 2. (a) AFM image of fluorographene. (b) Thickness of fluorographene sheets.

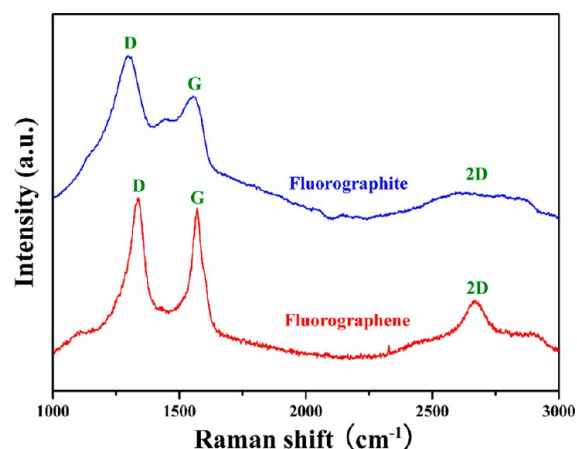


Figure 3. Raman spectra of pristine fluorographite and fluorographene.

of few-layer FG sheets.³⁴ In other words, the exfoliation of pristine fluorographite was successfully achieved.

FT-IR and ¹⁹F NMR characterizations were also carried out for acquiring more information about our product. Fluorographite exhibited a sharp peak at 1221 cm⁻¹ in its FT-IR spectrum (Figure S1, Supporting Information). This peak can be ascribed to the characteristic absorption of the C–F stretch.²⁴ The absorption peak of the C–F stretch for FG was located at 1217 cm⁻¹ with a slight red shift. This tiny distinction can be attributed to the different chemical environments of C–F bonds in fluorographite and FG. The exposure level of C–F bonds in FG is much higher than that in fluorographite. Therefore, the C–F stretch of FG needs less energy and this explanation is coincident with the red shift phenomenon. For ¹⁹F NMR, only FG showed a slight signal at –85.0 ppm in Figure S2 (Supporting Information) whereas fluorographite showed no signal. This result may be due to the different concentrations and specific surface areas of FG and fluorographite in NMP. As FG was prepared from fluorographite undergoing a large degree of exfoliation, the FG sheet was much thinner than the fluorographite particle and the specific surface area of a FG sheet was much bigger than that of a fluorographite particle. Thus, the dispersion of FG in NMP has a higher concentration and each FG sheet has many more F atoms exposed on the surface. Therefore, ¹⁹F signal of fluorographite cannot be detected by ¹⁹F NMR owing to its poor dispersity and small specific surface area.

To gain further structural information, both fluorographite and FG were characterized by XRD analysis (Figure 4). The (002) reflection of FG was very broad in comparison with that of pristine fluorographite, suggesting the poor ordering of FG sheets along the stacking direction. This phenomenon indicated that the FG sample comprised largely free FG sheets.³⁵ The (001) reflection peak at about $2\theta = 13.6^\circ$ demonstrated a hexagonal system compound with high fluorine content.³⁶

Thermal stability of the obtained FG was checked via a TGA investigation. The samples were heated from 40 °C to 750 °C in a N₂ gas stream with a heating rate of 10 °C/min. It can be found from Figure 5 that thermal stability of both fluorographite and FG was excellent below 400 °C, which is consistent with the previous report of Nair et al.¹⁴ In their earlier study, the loss of F for FG only became discernable for prolonged annealing above 400 °C.¹⁴ In the current case, the dramatic weight loss step of fluorographite took place from 500 °C whereas it occurred from 450 °C for FG. This phenomenon

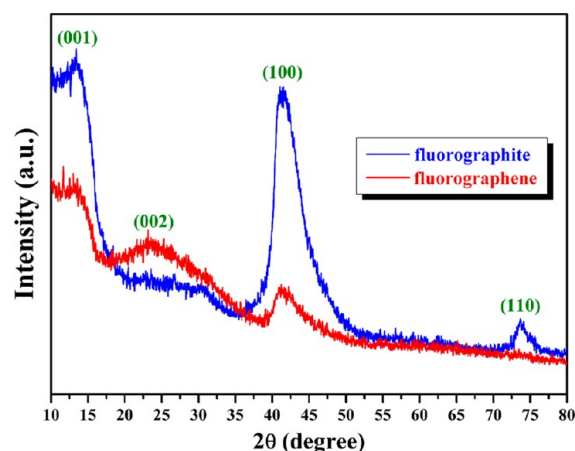


Figure 4. XRD patterns of pristine fluorographite and fluorographene.

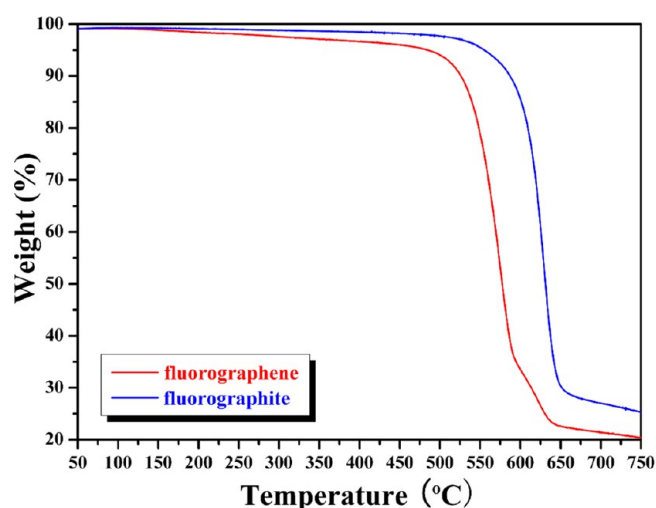


Figure 5. TGA (in N₂) thermograms of fluorographite and fluorographene with a heating rate of 10 °C/min.

can be attributed to the difference of specific surface area between fluorographite and FG. As all fluorographite particles are three-dimensional in scale and each particle is a multi-layer structure, the specific surface area of fluorographite is relatively small. Therefore, most C–C and C–F bonds are wrapped inside the particles and only a small part of them are exposed on the surfaces of particles. The chemical bonds wrapped inside the particles exhibit better thermal stability than those exposed on the surfaces of particles, which is why the dramatic weight loss step of fluorographite did not take place until 500 °C. Compared with fluorographite, our obtained FG sheets were two-dimensional in scale and each FG sheet was a few-layer structure, so the specific surface area of FG was much bigger than that of fluorographite. For FG, many more bonds were exposed on the surfaces of sheets than fluorographite particles (for monolayer FG, all bonds are exposed and none are wrapped). Thus, FG exhibited relatively poor thermal stability and its dramatic weight loss step occurred from 450 °C. In summary, both FG and fluorographite have good thermal stability and the thermal stability of FG is just slightly inferior to that of fluorographite.

To examine the electrochemical property, both FG and fluorographite were used as cathode materials of a primary lithium battery. The battery was discharged at a constant

current density of 100 mA/g. Discharge curves of fluorographite and fluorographene as cathode materials are shown in Figure 6. The specific discharge capacities of FG and

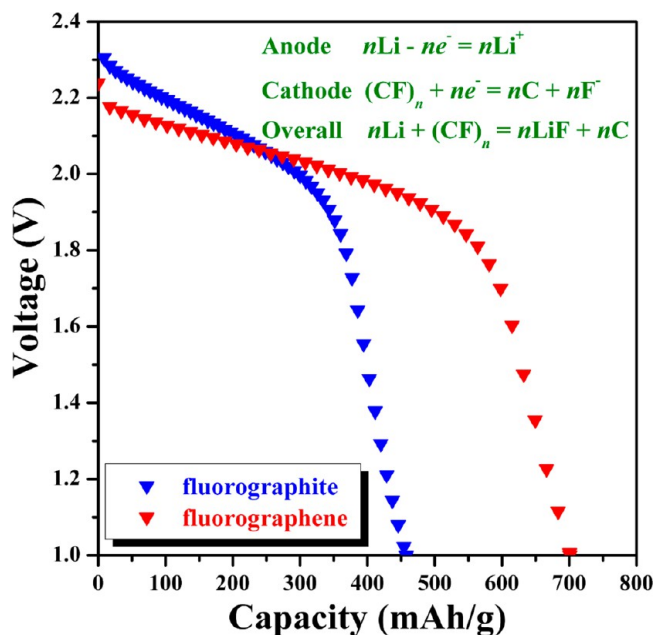


Figure 6. Discharge curves of fluorographite and fluorographene as cathode materials of a primary lithium battery with a current density of 100 mA/g.

fluorographene were 701.2 mAh/g and 457.9 mAh/g, respectively. Compared with fluorographite, it is obvious that the specific discharge capacity of FG improved significantly with a large growth of 53%. Because FG possesses much larger specific surface area than fluorographite, it is more favorable for Li^+ intercalating into FG than fluorographite. Therefore, FG had a much higher specific discharge capacity, which implied that FG is a promising cathode material.

To explore the potential application of FG in energy-storage devices of a capacitor, cyclic voltammetry (CV) was utilized to investigate the electrochemical property of the obtained FG. Figure 7 shows cyclic voltammograms of FG and fluorographite tested in 1 M Na_2SO_4 as an electrolyte. Scanning rates were 20, 40, 80, and 160 mV/s, respectively, and the potential range was from 0 to 1.0 V vs the $\text{Hg}/\text{Hg}_2\text{Cl}_2$ reference electrode. For FG, it should be noted that the areas of the closed curves under different scanning rates were dozens of times (30–80) bigger than that of fluorographite. As it is well-known, specific capacitance is proportional to the area of the closed cyclic voltammogram. As the scanning rate was just 20 mV/s, the specific capacitance of FG was 81.3 times of that of fluorographite; while the scanning rate was raised to 160 mV/s, the specific capacitance of FG was still 30.2 times of that of fluorographite. Combined with the results of discharge capacity of primary lithium battery, it can be clearly pointed out that the electrochemical properties were greatly improved with the generation of FG via the exfoliation of fluorographite.

4. CONCLUSIONS

In summary, we developed a new convenient approach of preparing fluorographene with a hexagonal polycrystalline structure via a quick exfoliation process from pristine fluorographite. The preparation process did not need heating,

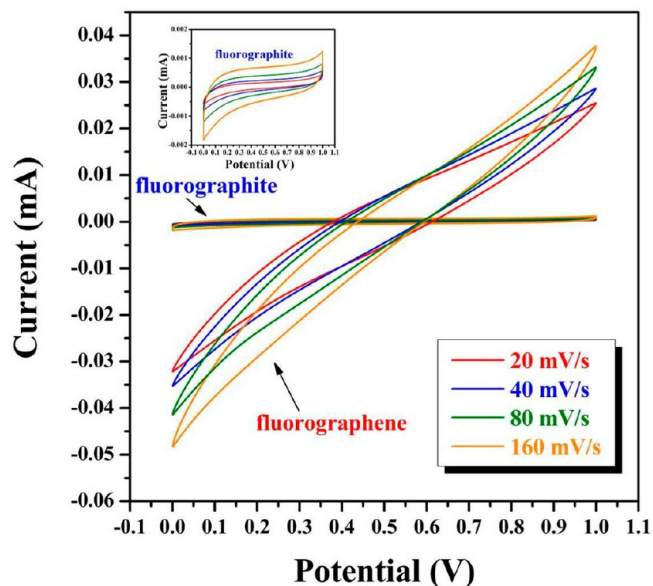


Figure 7. Cyclic voltammograms of fluorographite and fluorographene in 1 M Na_2SO_4 with different scanning rates.

sonication, and protective gas. This strategy for preparation of fluorographene is easy to implement, and it provides an easy-operating, highly scalable, and low-cost method for rapid preparation of few-layer FG using commercially available raw materials. FG is a promising cathode material of a primary lithium battery with a higher specific discharge capacity. Moreover, the specific capacitance of FG was dozens of times of that of fluorographite and the energy storage property of FG was rather excellent compared with fluorographite. As a promising 2D material, fluorographene has a bright prospect for application in many fields. Thus, we can believe that the industry is bound to need lots of demand for FG in the future and this work provides a viable solution to this great challenge.

■ ASSOCIATED CONTENT

Supporting Information

FT-IR and ^{19}F NMR spectra of fluorographite and fluorographene. This material is available free of charge via the Internet at <http://pubs.acs.org>.

■ AUTHOR INFORMATION

Corresponding Authors

*Y. Li. E-mail: liyongjun78@mail.sioc.ac.cn. Tel: +86-21-54925309. Fax: +86-21-64166128.

*X. Huang. E-mail: xyhuang@mail.sioc.ac.cn. Tel: +86-21-54925310. Fax: +86-21-64166128.

Notes

The authors declare no competing financial interest.

■ ACKNOWLEDGMENTS

The authors thank the financial supports from National Natural Science Foundation of China (21204098) and Shanghai Nano-Technology Program (11nm0501100).

■ REFERENCES

- Geim, A. K.; Morozov, S. V.; Jiang, D.; Zhang, Y.; Dubonos, S. V.; Grigorieva, I. V.; Firsov, A. A. *Science* **2004**, *306*, 666–669.
- Geim, A. K.; Novoselov, K. S. *Nat. Mater.* **2007**, *6*, 183–191.
- Geim, A. K. *Science* **2009**, *324*, 1530–1534.

- (4) Agrawal, S.; Frederick, M. J.; Lupo, F.; Victor, P.; Nalamasu, O.; Ramanath, G. *Adv. Funct. Mater.* **2005**, *15*, 1922–1926.
- (5) Novoselov, K. S.; Geim, A. K.; Morozov, S. V.; Jiang, D.; Katsnelson, M. I.; Grigorieva, I. V.; Dubonos, S. V.; Firsov, A. A. *Nature* **2005**, *438*, 197–200.
- (6) Berger, C.; Song, Z. M.; Li, X. B.; Wu, X. S.; Brown, N.; Naud, C.; Mayou, D.; Li, T. B.; Hass, J.; Marchenkov, A. N.; Conrad, E. H.; First, P. N.; de Heer, W. A. *Science* **2006**, *312*, 1191–1196.
- (7) Chen, H.; Muller, M. B.; Gilmore, K. J.; Wallace, G. G.; Li, D. *Adv. Mater.* **2008**, *20*, 3557–3561.
- (8) Gokus, T.; Nair, R. R.; Bonetti, A.; Bohmler, M.; Lombardo, A.; Novoselov, K. S.; Geim, A. K.; Ferrari, A. C.; Hartschuh, A. *ACS Nano* **2009**, *3*, 3963–3968.
- (9) Gu, Y.; Xu, Y.; Wang, Y. *ACS Appl. Mater. Interfaces* **2013**, *5*, 801–806.
- (10) He, H. K.; Gao, C. *ACS Appl. Mater. Interfaces* **2010**, *2*, 3201–3210.
- (11) Bhunia, S. K.; Jana, N. R. *ACS Appl. Mater. Interfaces* **2011**, *3*, 3335–3341.
- (12) Li, Z. F.; Zhang, H. Y.; Liu, Q.; Sun, L. L.; Stanciu, L.; Xie, J. *ACS Appl. Mater. Interfaces* **2013**, *5*, 2685–2691.
- (13) Geim, A. K.; Kim, P. *Sci. Am.* **2008**, *298*, 90–97.
- (14) Nair, R. R.; Ren, W.; Jalil, R.; Riaz, I.; Kravets, V. G.; Britnell, L.; Blake, P.; Schedin, F.; Mayorov, A. S.; Yuan, S.; Katsnelson, M. I.; Cheng, H. M.; Strupinski, W.; Bulusheva, L. G.; Okotrub, A. V.; Grigorieva, I. V.; Grigorenko, A. N.; Novoselov, K. S.; Geim, A. K. *Small* **2010**, *6*, 2877–2884.
- (15) Hong, X.; Cheng, S. H.; Herding, C.; Zhu, J. *Phys. Rev. B: Condens. Matter Mater. Phys.* **2011**, *83*, 085410.
- (16) Robinson, J. T.; Burgess, J. S.; Junkermeier, C. E.; Badescu, S. C.; Reinecke, T. L.; Perkins, F. K.; Zhalutdniov, M. K.; Baldwin, J. W.; Culbertson, J. C.; Sheehan, P. E.; Snow, E. S. *Nano Lett.* **2010**, *10*, 3001–3005.
- (17) Jeon, K. J.; Lee, Z.; Pollak, E.; Moreschini, L.; Bostwick, A.; Park, C. M.; Mendelsberg, R.; Radmilovic, V.; Kostecki, R.; Richardson, T. J.; Rotenberg, E. *ACS Nano* **2011**, *5*, 1042–1046.
- (18) Li, X.; Cai, W.; An, J.; Kim, S.; Nah, J.; Yang, D.; Piner, R.; Velamakanni, A.; Jung, I.; Tutuc, E.; Banerjee, S. K.; Colombo, L.; Ruoff, R. S. *Science* **2009**, *324*, 1312–1314.
- (19) Shivaraman, S.; Barton, R. A.; Yu, X.; Alden, J.; Herman, L.; Chandrashekar, M. V. S.; Park, J.; McEuen, P. L.; Parpia, J. M.; Craighead, H. G.; Spencer, M. G. *Nano Lett.* **2009**, *9*, 3100–3105.
- (20) Khan, U.; O'Neill, A.; Lotya, M.; De, S.; Coleman, J. N. *Small* **2010**, *6*, 864–871.
- (21) Li, D.; Muller, M. B.; Gilje, S.; Kaner, R. B.; Wallace, G. G. *Nat. Nanotechnol.* **2008**, *3*, 101–105.
- (22) Cheng, S. H.; Zou, K.; Okino, F.; Gutierrez, H. R.; Gupta, A.; Shen, N.; Eklund, P. C.; Sofo, J. O.; Zhu, J. *Phys. Rev. B: Condens. Matter Mater. Phys.* **2010**, *81*, 205435.
- (23) Withers, F.; Dubois, M.; Savchenko, A. K. *Phys. Rev. B: Condens. Matter Mater. Phys.* **2010**, *82*, 073403.
- (24) Zboril, R.; Karlicky, F.; Bourlinos, A. B.; Steriotis, T. A.; Stubos, A. K.; Georgakilas, V.; Safarova, K.; Jancik, D.; Trapalis, C.; Otyepka, M. *Small* **2010**, *6*, 2885–2891.
- (25) Gong, P. W.; Wang, Z. F.; Wang, J. Q.; Wang, H. G.; Li, Z. P.; Fan, Z. J.; Xu, Y.; Han, X. X.; Yang, S. R. *J. Mater. Chem.* **2012**, *22*, 16950–16956.
- (26) Chang, H.; Cheng, J.; Liu, X.; Gao, J.; Li, M.; Li, J.; Tao, X.; Ding, F.; Zheng, Z. *Chem.—Eur. J.* **2011**, *17*, 8896–8903.
- (27) Wang, Z. F.; Wang, J. Q.; Li, Z. P.; Gong, P. W.; Liu, X. H.; Zhang, L. B.; Ren, J. F.; Wang, H. G.; Yang, S. G. *Carbon* **2012**, *50*, 5403–5410.
- (28) Wang, X.; Dai, Y. Y.; Gao, J.; Huang, J. Y.; Li, B. Y.; Fan, C.; Yang, J.; Liu, X. Y. *ACS Appl. Mater. Interf.* **2013**, *5*, 8294–8299.
- (29) Lu, W. B.; Liu, S.; Qin, X. Y.; Wang, L.; Tian, J. Q.; Luo, Y. L.; Asiri, A. M.; Al-Youbicd, A. O.; Sun, X. P. *J. Mater. Chem.* **2012**, *22*, 8775–8777.
- (30) Chang, H. X.; Sun, Z. H.; Yuan, Q. H.; Ding, F.; Tao, X. M.; Yan, F.; Zheng, Z. J. *Adv. Mater.* **2010**, *22*, 4872–4876.
- (31) Stankovich, S.; Dikin, D. A.; Piner, R. D.; Kohlhaas, K. A.; Kleinhammes, A.; Jia, Y.; Wu, Y.; Nguyen, S. T.; Ruoff, R. S. *Carbon* **2007**, *45*, 1558–1565.
- (32) Wu, Z. S.; Pei, S. F.; Ren, W. C.; Tang, D. M.; Gao, L. B.; Liu, B. L.; Li, F.; Liu, C.; Cheng, H. M. *Adv. Mater.* **2009**, *21*, 1756–1760.
- (33) Nuvoli, D.; Valentini, L.; Alzari, V.; Scognamiglio, S.; Bon, S. B.; Piccinini, M.; Illescas, J.; Mariani, A. *J. Mater. Chem.* **2011**, *21*, 3428–3431.
- (34) Withers, F.; Dubois, M.; Savchenko, A. K. *cond-mat.mtrl-sci*, arXiv: 1005.3474v3 (September 6, 2010).
- (35) Nethravathi, C.; Rajamathi, M. *Carbon* **2008**, *46*, 1994–1998.
- (36) Hamwi, A. J. *Phys. Chem. Solids* **1996**, *57*, 677–688.